British Journal of Cancer Research
2020; 3(1): 341 - 348. doi: 10.31488/bjcr.141

Research article

# Immune Attack against Breast Cancer Revealed in Patient Tumor Sections by Memristive Nanowire Sensors

Abuduwaili Tuoheti[&1], Angélique Pabois[&2], Francesca Puppo[3], Isaac Crespo[4], Ioulia Tzouvadaki[3], Danilo Demarchi[1], Jean-François Delaloye[5], Ioannis Xenarios[4], Sandro Carrara[3] and Marie-Agnès Doucey[*2]

1. Politechnico di Torino, Corso Duca degli Abruzzi, 24, 10129 Torino, Italy

2. Ludwig Institute for Cancer Research, Lausanne Branch, Chemin des Boveresses 155, CH1066 Epalinges, Switzerland

3. EPFL, INF 338, Station 14, CH1015 Lausanne, Switzerland

4. CHUV, Agora Center, Bugnon 25A, 1005 Lausanne

5. Centre du sein, CHUV, Avenue Pierre Decker 2, CH 1011 Lausanne, Switzerland

[*]Corresponding author: Dr. M.A. Doucey, Ludwig Institute for Cancer Research, Lausanne Branch, Chemin des Boveresses 155, CH1066 Epalinges, Switzerland, E-mail: marie-agnes.doucey@unil.ch

&Equal Contribution

Received: November 10, 2019; Accepted: December 03, 2019; Published: December 10,

## Abstract

A foundational principle of tumor immunology is that cancer cells can be eliminated by host cytotoxic T lymphocytes. This T lymphocyte immune attack can be potentiated by novel treatment modalities called immunotherapies and, patient tumors with pre-existing immune attack are more responsive to immunotherapies. However, cancers often hijack immune attack and precision oncology seeks for decision-making tools that are able to identify immune attack in minute amounts of patient tumor biopsies. Silicon nanowire memristive sensors for biodetection are the latest generation of nanowire sensors. They have marked a new era with unprecedented detection of attomolar to femtomolar concentrations of biomolecules. Here, we have designed memristive nanowire sensors for the first ever detection of immune attack in a five micrometers section of breast cancer patient tumor biopsy. In the momentum of breast cancer immunotherapy, these sensors emerge as a technological breakthrough that has the potential to guide precision medicine in oncology.

**Keywords:** nanowires, memristive sensors, immune attack, breast cancer patients, precision medicine

## Introduction

Breast Cancer (BC) is the most common type of cancer and the leading cause of cancer death in women. BC is recognized as a heterogeneous malignancy and, over the years, considerable efforts have focused on understanding the molecular bases of this heterogeneity and contributed to improve therapies [1]. Immunotherapies are novel treatment modalities that aim to provoke immune attack against cancer and, currently, multiple ongoing clinical trials evaluate immunotherapy strategies for patients with BC [2, 3]. With the recent success of BC immunotherapies [2, 3], it becomes increasingly relevant to understand which patient can benefit from immunotherapies, conventional therapies (chemotherapy, radiotherapy and targeted therapy) or combination of both. Individual BC patients with ongoing active immune attack are more likely to benefit from immunotherapy and, their immune system more easily mobilized against cancer relative to patient tumor without detectable immune attack. However, currently, precision medicine in immuno-oncology lacks decision-making tool able to guide therapeutical decision by quantifying active immune attack in minute amounts of patient tumor biopsies. Over the past six years, silicon nanowire (SiNW) sensors have undergone unprecedented development in the field or cancer [4] with the emergence of devices with outstanding sensitivities [5]. However, these sensors remain yet in an early phase of detection of clinical specimens limited to soluble markers and miRNA in serum[6, 7] and, volatile organic compounds in the exhaled breath of cancer patients [8, 9].

In 2011, we have pioneered SiNW memristive sensors for biodetection [10] and reported their unprecedented Limit-of-Detection (LoD) of attomolar to femtomolar concentrations of cancer-related biomolecules in a simple controlled environment and serum [11-16]. Further, we have developed SiNW memristive sensor chips for multiplexed detection that are perfectly integrated into clinically meaningful portable point-of-care diagnostic devices [17, 18]. Now, we report here the first ever detection of immune attack in a five micrometers section of BC patient tumor biopsy with NW memristive sensors. This technological breakthrough can help delineating BC patients who can benefit from immunotherapies and emerge as the first decision-making tool for precision immuno-oncology.

### In Air High Sensitivity Biodetection with Memristive NW Sensors

SiNW memristive sensors have been successfully used for biodetection [10] and are two-electrode (Source and Drain)

systems with Schottky barrier junctions (JL and JR) that confer hysteretic properties to a polycrystalline SiNW functionalized with antibodies (Figure 1A and Figure S1). SiNW memristors operate at higher sensitivity (aM-fM range [11, 14]) than SiNW field effect transitor (FET) sensors (fM-nM range [4]) owing to their detection in air that limits the shielding effect of soluble positively charged ions accumulated around the antibody-antigen complex (Figure 1A). Consequently, Debye length [19] and detection sensitivity are increased (Figure 1A). SiNW memristive sensors measure antibody-antigen interaction as changes in the memristive conductivity reflected by quantitative variations in the voltage gap (Vgap) of the hysteresis curve (Figure 1B). Upon functionalization, a Vgap appears in the NW memristive conductivity (Figure 1B) that is inversely proportional to the concentration of the detected antigen in solution [4, 10, 11, 14].

In breast [20] and other cancers, upon immune attack, T lymphocytes and natural killer (NK) cells produce and release the tumor cell death-inducing enzyme granzyme (GRA)[21] and interferon-γ (IFN-γ), a pluripotent anti-tumor cytokine largely implicated in the success of immunotherapies [22]. However, while both T and NK cells can kill tumor cells, only T cells encompass memory cells that ensure long lasting immune protection [23]. Thus, both the density of tumor infiltrating lymphocytes (TILs)[20] and tumor cell killing capability determine the strength of immune attack and correlate with clinical outcome of BC patients [24].

**Detection of T Cell Immune Attack with Memristive NW Sensors**

To detect immune attack, we have designed a NW chip composed by two series of six wire arrays for multiplexed detection of GRA and IFN-γ (Figure S2). We first detected immune attack in T lymphocytes isolated from donor peripheral blood and activated in vitro by triggering of their T cell receptor (TCR) and co-receptor CD28 (Figure. S3A). This type of activation is independent of the specificity of the TCR and induced by clustering of the TCR at the T cell surface by ligation with the antibody. This activation is further amplified by ligation of CD28, the major T cell co-stimulatory molecule. The later acts as an amplifier of TCR stimulation and can be triggered with CD28-specific antibodies. Thus, anti-TCR and anti-CD28 antibodies were used to trigger CD8 T cell activation in vitro. Activated T cells release GRA and IFN-γ in the culture medium that we quantified with NW sensors or a commercially available bead cytokine array. NW sensors and bead array detected IFN-γ secretion equivalent to 5 and 1000 T cells, respectively (Figure 1C). We determined that the concentration of IFN-γ in the conditioned medium of 1000 T cells was 250 fM i.e. 1.25 fM for 5 T cells. We next exposed directly to NW sensors as few as 6 or 12 T cells (Figure S3B) and detected significantly higher levels of GRA in activated T cells relative to non-activated ones (Figure 1D). Consistently, flow cytometry analysis of 100 000 T cells of the same culture revealed basal levels of GRA secretion in non-activated T cells and an activation-induced T cell immune attack (Figure 1D).

**Quantification of Immune Attack in BC Patient Tumor Section**

These outstanding performances prompted us to detect, for the very first time, immune attack in sections of patient tumor biopsies. In clinical settings, the later are subjected to histopathological characterization to assess tumor grade (i.e. the degree of tumor cell growth and differentiation), which along with the extent of cancer spreading, support treatment decision. We first ensure that antibody-functionalized wires withstand proteases that are released by tumors to promote cancer cell spreading (Figure S4A). Next, we evaluated the sensor detection performances in patient tumor specimens by using NW sensors functionalized with anti-rabbit immunoglobulin antibodies for the detection of exogenously spiked rabbit immunoglogin G in extract of breast carcinomas (Figure 2A, left panel). Significant variations in Vgap detected in the presence of 100 fM of rabbit immunoglobulin, but not in its absence, confirmed specific detection at high sensitivity (Figure 2A, right panel) with a specific signal 5-fold above the noise signal (measured in the absence of rabbit immunoglobulin). We next contacted a frozen section of BC with a drop of phosphate buffer saline (PBS) for 15 min at room

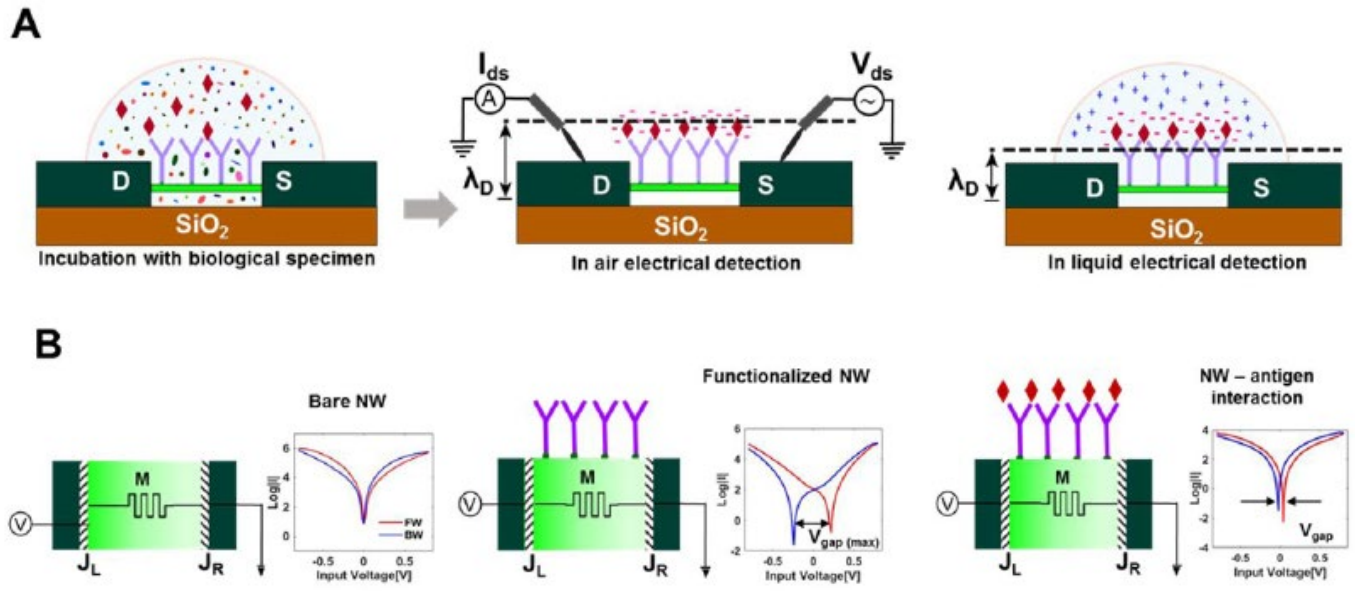

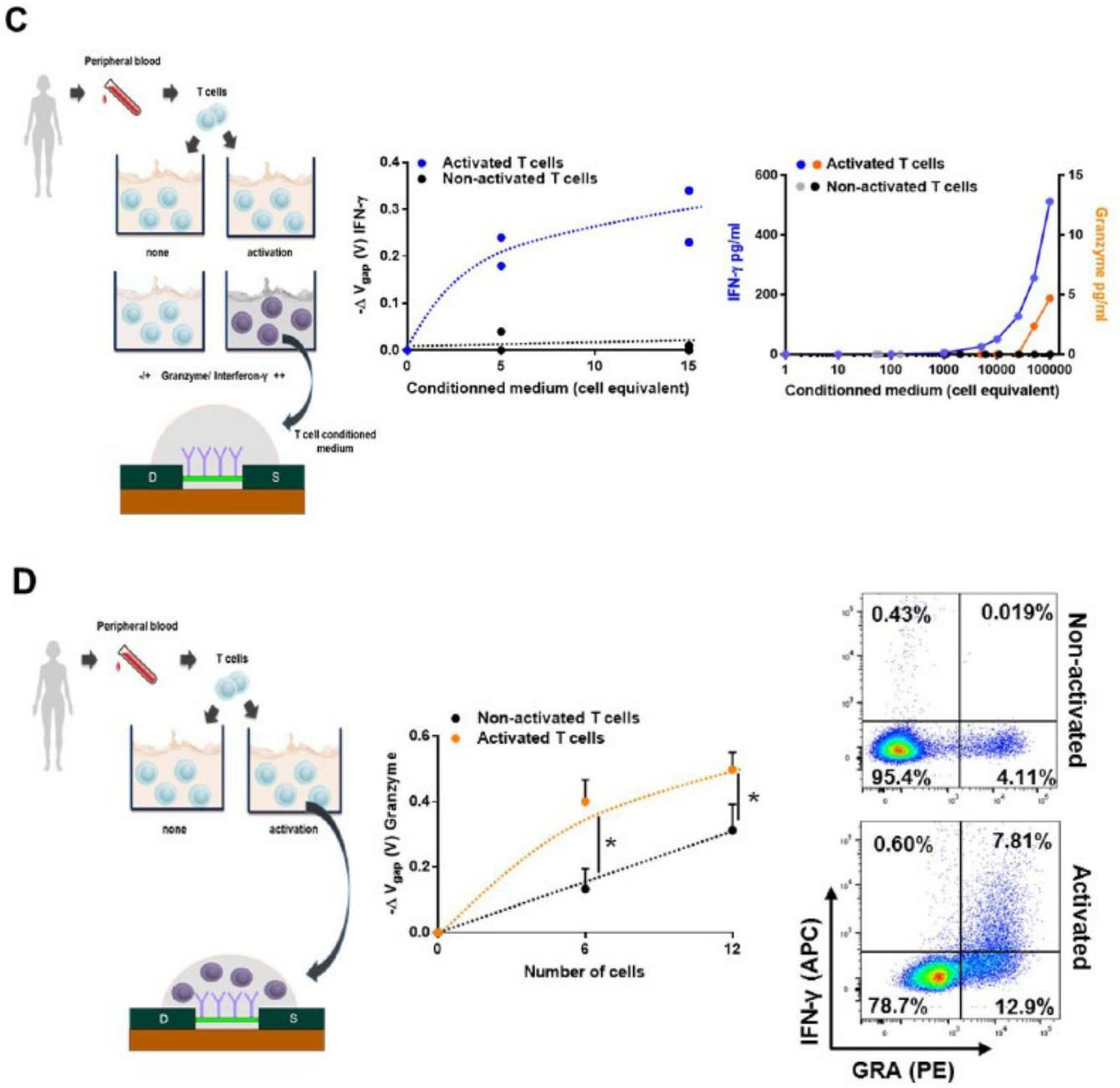


**Figure 1.** High sensitivity detection of immune attack in T lymphocytes with memristive NW sensors. (A) Principle of operation of memristive sensor with biological specimens, SiNW (green) functionalized with antibodies (purple) and connected to source (S) and drain (D). NW immobilized-antibodies interact specifically with soluble antigens (red diamonds) of the biological specimen. In air (NW memristor) and in liquid (FET NW sensor) electrical detection schemes and their effects on Debye length ($\lambda_D$). (B) Schematics of memristive sensor and variations of drain-source current ($I_{ds}$-$V_{ds}$ curves) recorded in bare, antibody-functionalized NW interacting or not with antigen. M: electrical equivalent component of a memristor; $V_{gap}$: voltage gap; forward (FW, red) and backward (BW, blue) branches of the hysteresis curve. (C) CD8 T lymphocytes were isolated from healthy donor peripheral blood and activated in vitro through polyclonal stimulation of their T cell receptors (TCR) with anti-TCR/CD3ε and anti-CD28 stimulatory antibodies. CD8 T lymphocytes are killer cells that produce and secrete gran zyme and IFN-γ to kill target cells and to mount immune response, respectively. Detection of GRA and IFN-γ with NW memristive sensors (left, duplicated detection) or a commercial cytokine bead array (right) in the conditioned medium of T cells activated in *vitro*. (D) Similarly as in (C), CD8 T cells were stimulated in vitro for 5 hours and the whole culture (T cells and conditioned medium) applied to NW sensor.Detection of GRA and IFN-γ in activated T cells following directly exposure to NW sensors (left) or staining and detection by flow cytometry (right). Each measurement was performed with 5-6 wire arrays. Data are mean ± SEM, unpaired t-test.

temperature and exposed the contacted liquid to NW sensors to quantify GRA and IFN-γ (Figure 2B). Subsequently, these sections were processed for quantification of TILs by immunohistochemistry (Figure 2B and Supplementary Figure 4B). As expected, changes in Vgap related to GRA and IFN-γ increased with the fraction of the liquid that contacted the tumor tissue section (Figure 2C). As a proof of concept, we selected two tumors (A and B) with high and low histological grade, respectively. Immune attack, as reflected by GRA detected into the sections with NW sensors, was significantly higher in tumor B relative to A. Gelatin-functionalized NW, used as a negative control, show that tumor A contained very low but detectable amounts of GRA (Figure 2D). Subsequent quantification of TILs in these tumor sections by immunofluorescence microscopy (Figure 2E) revealed significantly lower TIL counts in tumor A relative to tumor B, which mirrored the extent of immune attack against the tumor (Figure 2F). Examination of GRA and TCR/CD3e gene expression in breast tumors at time of diagnosis in a cohort of 947 patients revealed that high immune attack against cancer (as observed in 40% of the tumors shown in orange, Figure 2G) was associated with a significantly longer survival, especially at two years post-diagnosis (Figure 2H).

Memristive sensors have the potential to identify individual BC patients with ongoing active immune attack that are more likely to benefit from immunotherapy. This study reports the first detection of cancer analytes at ultra-high sensitivity from patient tumor specimens using memristive NW sensors. Because memristive NW sensors can be functionalized with any antibody and operate with sections of tumor tissue biopsies that are widely used in clinical practice, they emerge now as decision-making tool for precision oncology. Hence, the ability of NW memristive sensors to quantify immune attack or other molecular features in patient tumor represents a first step toward precision medicine, and their integration into portable devices has the potential to revolutionize cancer diagnosis and patient monitoring. However, to date, several obstacles have hinder their development into clinically meaningful portable point-of-care devices. They need to withstand the complex matrix of biological specimens, to overcome their currently limited multiplex detection capabilities and, to match robust performance metrics of detection. We have achieved a robust functionalization of SiNW that withstand the proteolytic activity of tumor proteases by using a covalent attachment of antibodies to the NW and by an alternative scheme of analyte detection in air that also limits proteolytic activity. Further, we have reached the highest level of multiplexed detection reported to date for NW sensors [4]. Given the observed fluctuations in sensing, multiple detection of the same analyte is needed to reach statistical significance [25] thus limiting sensor multiplex capability. However, in marked contrast to functionalization and detection schemes in liquid, in air functionalization and detection are more robust, more sensitive and do not require sensor integration into micro-fluidic systems. Hence, because they can be easily multiplexed and represent a path towards clinical applications, in air functionalization and detection schemes should be encouraged. Finally, memristive siNW sensors will transition from this early phase of target detection in complex patient clinical specimens to in vitro diagnostic and prognostic devices after they meet regulatory requirements and performance metrics of detection. This will be achieved by more uniform NW fabrication and improved functionalization processes currently under development in our groups.

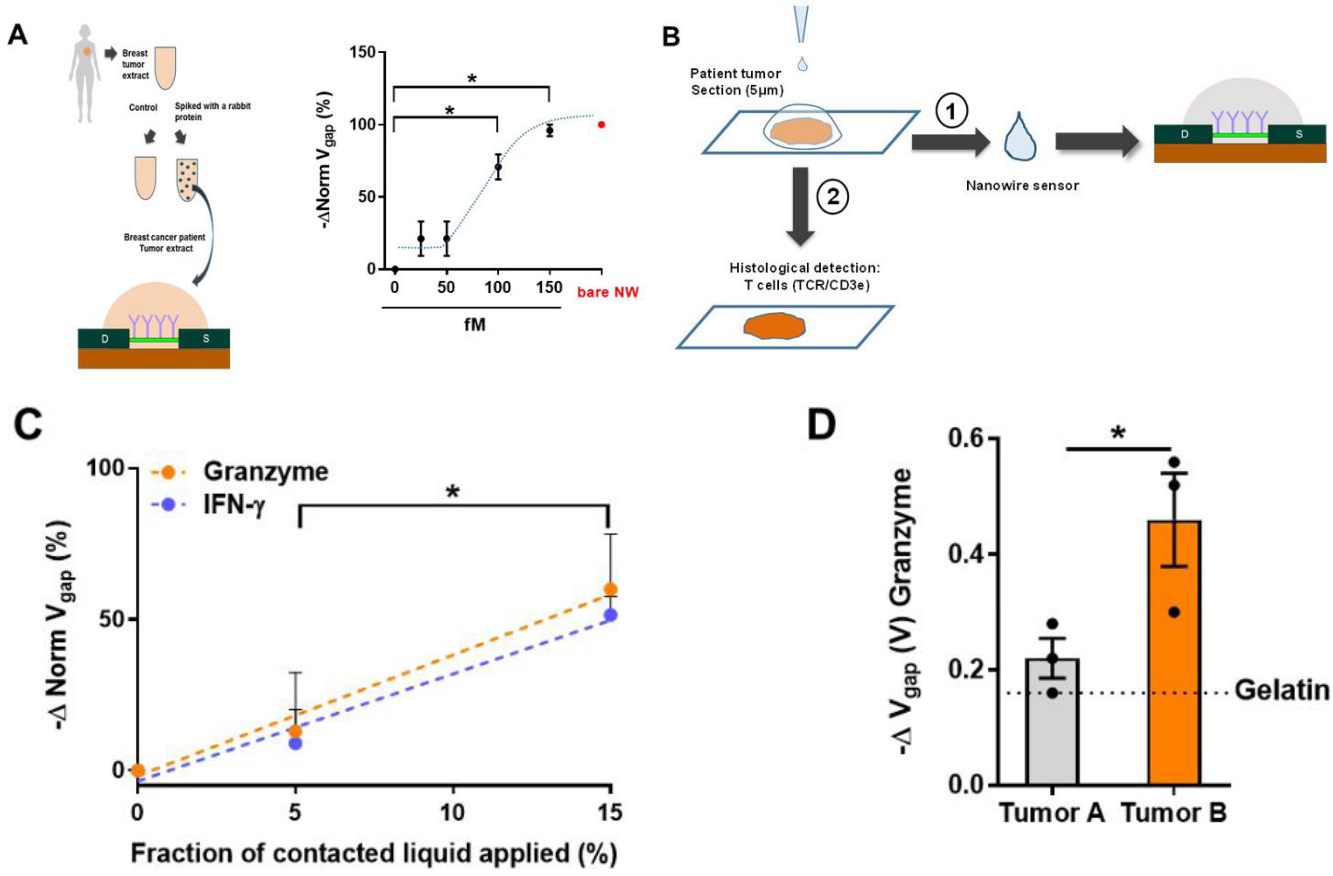

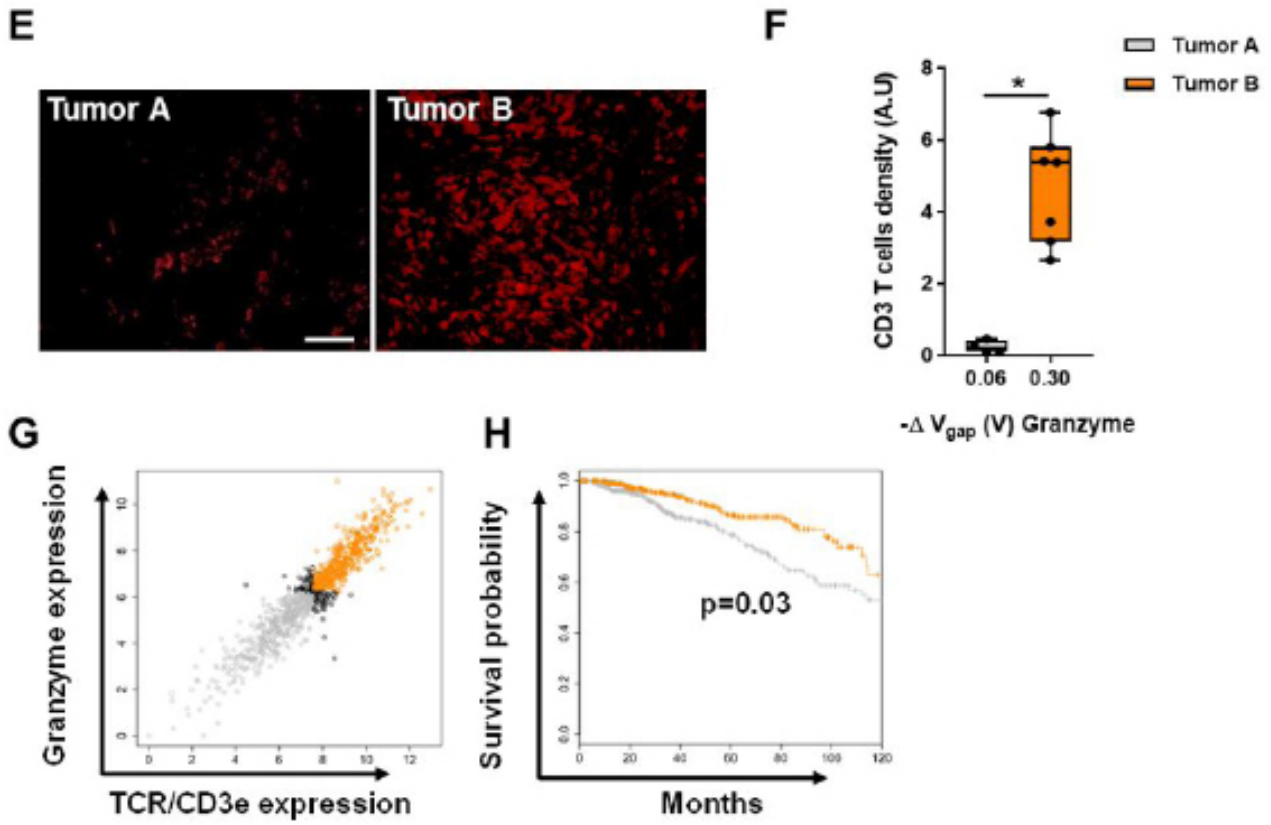


**Figure 2.** BC patient stratification based on quantification of immune attack in tumor section with NW memristive sensors. (A) Left: A patient breast tumor extract was supplemented or not (control) with known fM concentrations of a rabbit immunoglobulin G and the mixtures exposed to NW sensors functionalized with antibodies specific for rabbit immunoglobulin G. Right: specific detection with NW sensors of rabbit immunoglobulin spiked in breast tumor tissue extracts. Data are mean ± SEM, Kruskall Wallis test with Dunn's post-test. (B) Frozen sections of tumor tissues placed on glass microscopy slides were contacted for 15 min at room temperature with PBS, the contacted liquid was collected and applied to NW sensors functionalized with antibodies specific for GRA and IFN-γ (C-D). Subsequently, the tumor sections were used for immunohistological characterization (E). (C) Measure of GRA and IFN-γ with NW sensors in diluted fractions of the liquid contacted with a frozen sections of tumor tissue, data are mean ± SEM, unpaired t-test. (D) Likewise in (C), GRA was measured in the liquid contacted with sections from tumors with high (A) and low (B) histological grade. Gelatin-functionalized wires were used as a negative control. Each measurement was performed with 4 wire arrays. Data are mean ± SEM, unpaired t-test. (E) TILs in sections of the same tumors detected by immunofluorescence microscopy. Bar: 12 µm. (F) Quantification of immune attack in tumor A and B by combining GRA (NW sensor) and CD3 density (immunohistochemistry) measurements. Data are mean ± SEM, unpaired t-test. (G) Distribution of GRA and TCR/CD3 gene expression in 947 BC from The Cancer Genome Atlas (TCGA) database. Orange and gray colors delineate patient tumors with high and low-intermediate gene expression of TCR/CD3 and GRA, respectively. (H) Corresponding patient relapse free survival.

## Experimental Section

### Patients, tissue specimens and breast tumor extracts

This study has been approved by the ethics committee of the Canton of Vaud, Switzerland. Patient tissue specimens were obtained according to the declaration of Helsinki and upon written informed consent. All patient tumors were invasive ductal carcinoma of the breast with histological grade (Elston and Ellis) ranging from I to III and with T1 to T3 tumors. Patients were treatment naive at time of tumor collection (age 38-60 years old) with no distant metastasis but to the lymph node (50% of them). Tumor A is a grade III triple negative invasive ductal carcinoma (T2, N1a) while tumor B is a luminal A invasive ductal carcinoma of grade II (T2, N3). Breast tumor biopsies from 6 distinct invasive ductal breast carcinoma were snap frozen in liquid N2, pooled and grinded down to tissue powder with a mortar and a pestle, resuspended in sterile water and further homogenized with a tip sonicator on ice. The resulting tumor extract was clarified by centrifugation and the protein concentration adjusted to 1 mg/ml.

### Process flow for SiNW fabrication

The SiNW were fabricated on SOI (Silicon-On-Insulator) wafers using a top-down process based on a deep reactive ion etching (DRIE) technique developed in our group [15, 26-28]. First, E-Beam lithography (EBL) draws major features on a polymeric resist followed by Ni deposition and lift-off processes thus forming Ni contact pads on Si oxide with a 500 nm gap in between. Multiple annealing steps at high-temperature create Nickel Silicide. Then, a second EBL mask patterns nano-scale slabs on a high resolution resist (Hydrogen SilselsQuioxane - HSQ) used as hard-mask for the following DRIE process that chemically erodes the Si layer creating scalloped-trenches and, in the end, free-standing, vertically- stacked SiNWs bridging the Ni contacts. Metal lines composed of Platinum (Pt) are fabricated as electrode extension to the NiSi contacts [17]. This whole process results in chips made of 12 integrated sensors (each one

composed of 4 vertically-stacked NW) with individual drains (D) and one common source (S) (Supplementary Figure 2).

**NW Surface functionalization for immuno-detection**

The SiNWs were functionalized by covalent attachment of antibodies with glycidoxypropyltrimethoxysilane (GPTS). After treatment with Piranha solution or oxygen plasma (Harrick oxygen plasma, 200mTorr, 29W), the Si substrate was incubated in ethanol containing 10 mM acetic acid and 1% GPTS. The surface was dried under a N2 stream and then exposed to 95 °C for 15 min in a dry oven. Antibodies (anti-interferon gamma: Biolegend, clone MD-1, 507501; anti-human Granzyme A: Biolegend, clone CB9, 507202 and fish gelatin used as a negative control) were spotted at 0.5mg/ml in PBS containing 0.5% trehalose using a non-contact piezoelectric Nano-Plotter (GeSim2.1) at the Protein Analysis Facility of the University of Lausanne. Spotting of the antibodies onto individual wires of the Si chip was controlled by observation with a microscope. The printing scheme is shown on Supplementary Figure 2A. The chip surface was then washed with 10% PBS and the remaining active GPTS groups were blocked by incubation in a solution of 10 mM of ethanolamine (pH 8.0) for 60 min at room temperature. Finally, the functionalized NW were blocked by an additional incubation in PBS containing 3% gelatin from cold water fish skin. The modified surface was rinsed with PBS and stored in PBS at 4°C until use. Chemicals unless stated otherwise were purchased from Sigma-Aldrich (St-Louis, MO).

**Immunoblotting**

Tumor extracts were prepared as described above. Protein concentration was determined using BCA™ protein assay reagent (ThermoFischer Scientific). Tumor extracts were then resolved by SDS-PAGE (12%) (ThermoFischer Scientific), and proteins were transferred to PVDF membranes (ThermoFischer Scientific) using an iBlot semidry electrophoretic transfer device (Life technologies). Then, membranes were subjected to immunoblot analysis. Antibody-bound proteins were detected using an enhanced chemiluminescence kit (Advansta, Menlo Park, CA, USA) and luminescent image analyzer Fusion FX (Vilber Lourmat, Marne-la-Vallée, France). Image analyses and blot quantification were performed with FusionCapt Advance software (Vilber Lourmat). Results shown are representative of 6 different tumor extracts.

**Experimental protocol for sensing**

Memristive NW sensors were exposed to biological specimens by incubation for 30 min at RT under 50% humidity. Biological specimens include T lymphocyte conditioned medium, suspension of T lymphocytes, breast tumor extracts and PBS that contacted sections of BC patients. All incubations were of 30 min at RT but tumor extracts and PBS that contacted tumor sections that were limited to 15 min. Then, the sensor was washed three times with PBS to remove non-specific interactions and once with 10% PBS to lower salt concentration. The sensor were gently dried under N2 flow, and loaded into the custom developed portable low power electronic system.[29] The memristive biosensor chip was plugged into the electronic system to acquire data for the source-to-drain current-voltage (Ids-Vds) curves and to monitor the hysteretic Vgap.

**Isolation of human CD8+ T cells, flow cytometry and cytokine secretion**

Total peripheral blood mononuclear cells (PBMC) were anonymous samples obtained from healthy donors (Transfusion Inter-regionale CRS, Canton of Vaud, Switzerland)). CD45RA-CD8+ T cells were isolated using human CD8+ T cell Isolation kit (Miltenyi Biotec, Bergisch Gladbach, Germany) and then activated in 96-well plates coated with anti-human-TCR/CD3e (clone OKT-3 Biolegend, San Diego, CA) and anti-human-CD28 (clone CD28.2 Biolegend). T cell conditioned medium or cells were collected post-activation and applied onto the NW sensors for granzyme or interferon-γ detection. Alternatively, for the detection of granzyme and interferon-γ-producing cells by flow cytometry, Golgi Stop (BD Biosciences, Franklin Lakes, NJ) was added to the culture 5 hours prior to the cell harvest to accumulate cytokine in the Golgi apparatus by preventing the secretion of cytokines in the culture medium. After an aqua live/dead staining (Thermo Fischer Scientific, Waltham, MA) CD8+ T cells were stained for surface markers (anti-human CD3-Bv421 (Biolegend) and anti-human CD8-FITC (Bioloegend)) with antibodies followed by fixation and permeabilization (Fixation & Permeabilization Buffer Set, Thermo Fischer Scientific). Cells were then stained intracellularly for human granzyme A (BD Biosciences) and human IFN-γ (BD Biosciences) and cell-associated fluorescence acquired with a FACS LSR II® (BD Biosciences) and analyzed using FlowJo® 10 software (Tree Star, Inc., Ashland, OR) (Supplementary Figure 5). Secreted granzyme and IFN-γ were measured and quantified in cell conditioned medium of human CD8+ T cells using the Cytometric Bead Array (CBA) (BD Biosciences) as previously described [30, 31].

**Histology, immuno-fluorescence and microscopy**

Snap frozen primary BC specimens were cut in 5 µm sections with a microtome following embedding into Optimal Cutting Temperature compound (Tissue-Tek® O.C.T.), stained and imaged as previously described[32] using a Zeiss Axiovision microscope (Zeiss LSM510, Oberkochen, Germany).

**Analysis of BC patient survival based Granzyme A and CD3ε gene expression levels**

Gene expression from 1096 breast tumors from TCGA-BRCA dataset, publicly available at the NIH: National Cancer Institute, GDC Data Portal (WWW://portal.gdc.cancer.gov/repository) were used for analysis. The expression data were RSEM normalized [33] and Log2 transformed. The overall survival time of the related patients corresponds to a manually curated version of the TCGA-BRCA [34] dataset which was transformed from days into months (30.5 days/month). The statistical significance of the survival separation between the two groups of patients was calculated by performing a log-rank statistic using Terry R package survival.

**Statistics**

Statistical analyses were performed using GraphPad Prism V7.03 (San Diego, CA). The data are expressed as mean ± SEM and compared using unpaired t-test or Kruskal-Wallis test

(with Dunn's multiple comparison post-test) if there were more than two conditions. Results were considered to be significant with *p<0.05.

The Table of Contents

Memristive nanowire sensor enable the first ever direct detection of immune attack in a five micrometers section of breast cancer patient tumor tissue. Immunotherapies are novel treatment modalities that aim to provoke attack of the immune system against cancer. Memristive sensors capable of sensing immune attack represent the first decision-making tool able to delineate patients that can benefit from immunotherapies (Figure 3).

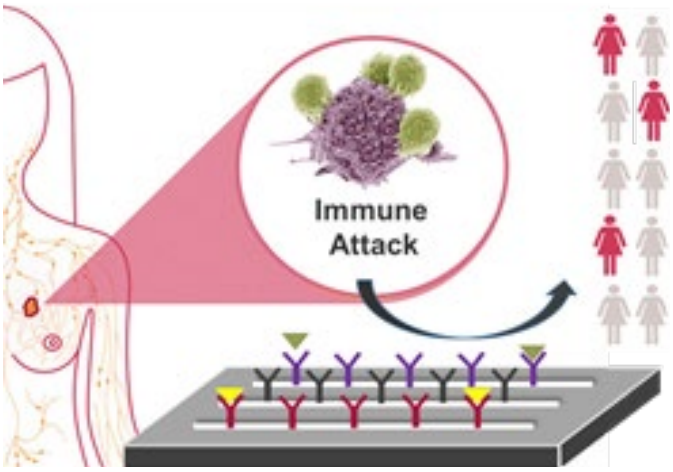


**Figure 3.** ToC figure.

Acknowledgements

We thank Dr Manfredo Quadroni and Séverine Lorrain (Protein Analysis Facility, University of Lausanne) for printing the antibodies onto the wire chips. This work was supported by grants from the Swiss National Foundation (M.-A. Doucey, project 310030-120473) and the Medic foundation (M.-A. Doucey). A. Tuoheti and A. Pabois contributed equally to this work.

## References

1. Cardoso F, van't Veer LJ, Bogaerts J, et al. 70-Gene Signature as an Aid to Treatment Decisions in Early-Stage Breast Cancer. NEJM. 2016; 375 (8): 717-729.
2. Monnot GC, Romero P. Rationale for immunological approaches to breast cancer therapy. Breast. 2018; 37: 187-195.
3. Zacharakis N, Chinnasamy H, Black M, et al. Immune recognition of somatic mutations leading to complete durable regression in metastatic breast cancer. Nat Med. 2018; 24 (6): 724-730.
4. Doucey MA, Carrara S. Nanowire Sensors in Cancer. Trends Biotechnol. 2019;37(1):86-99.
5. Salvati E, Stellacci F, Krol S. Nanosensors for early cancer detection and for therapeutic drug monitoring. Nanomedicine. 2015; 10 (23): 3495-3512.
6. Lee MH, Lee DH, Jung SW, et al. Measurements of serum C-reactive protein levels in patients with gastric cancer and quantification using silicon nanowire arrays. Nanomed Nanotechnol. 2010; 6 (1): 78-83.
7. Gao A, Yang X, Tong J, et al. Multiplexed detection of lung cancer biomarkers in patients serum with CMOS-compatible silicon nanowire arrays. Biosens Bioelectron. 2017; 91: 482-488.
8. Krilaviciute A, Heiss JA, Leja M, et al. Detection of cancer through exhaled breath: a systematic review. Oncotarget. 2015; 6 (36): 38643-38657.
9. Shehada N, Brönstrup G, Funka K, et al. Ultrasensitive silicon nanowire for real-world gas sensing: noninvasive diagnosis of cancer from breath volatolome. Nano Lett. 2015; 15 (2): 1288-1295.
10. Sacchetto D, Doucey MA, De Micheli G, et al. New Insight on Bio-sensing by Nano-fabricated Memristors Bio Nano Science. 2011; 1 (1-2): 1-3.
11. Puppo F Dave A, Doucey MA, et al. Memristive Biosensors Under Varying Humidity Conditions. IEEE Trans Nanobioscience. 2014; 13 (1):19-30.
12. Puppo F, Doucey MA, Di Ventra M, et al. Memristor-based devices for sensing. In 2014 IEEE International Symposium on Circuits and Systems (ISCAS), 2014; 2257-2260.
13. Tzouvadaki I, Madaboosi N, Soares RRG, et al. Bio-functionalization study of Memristive-Biosensors for early detection of prostate cancer&#x201D. In 2015 11th Conference on Ph.D. Research in Microelectronics and Electronics (PRIME), 2015; 17-20.
14. Tzouvadaki I, Jolly P, Lu X, et al. Label-Free Ultrasensitive Memristive Aptasensor. Nano Letters. 2016; 16 (7): 4472-4476.
15. Puppo F, Doucey MA, Delaloye JF, et al. SiNW-FET in-Air Biosensors for High Sensitive and Specific Detection in Breast Tumor Extract. IEEE Sensors J. 2016; 16 (10): 3374-3381.
16. Puppo F, Doucey MA, Delaloye JF, et al. High sensitive detection in tumor extracts with SiNW-FET in-air biosensors. In IEEE SENSORS 2014 Proceedings. 2014; 866-869.
17. Tzouvadaki I, Tuoheti A, De Micheli G, et al. Portable Memristive Biosensing System as Effective Point-of-Care Device for Cancer Diagnostics. In 2018 IEEE International Symposium on Circuits and Systems (ISCAS), 2018; 1-5.
18. Tzouvadaki I, Tuoheti A, Lorrain S, et al. Multi-Panel, On-Single-Chip Memristive Biosensing. IEEE Sensors J. 2019; 1-1.
19. Stern E, Wagner R, Sigworth F, et al. Direct Ultrasensitive Electrical Detection of DNA and DNA Sequence Variations Using Nanowire Nanosensors. Nano Letters. 2007; 7 (11): 3405-3409.
20. Wein L, Savas P, Luen S, et al. Clinical Validity and Utility of Tumor-Infiltrating Lymphocytes in Routine Clinical Practice for Breast Cancer Patients: Current and Future Directions. Front Oncol. 2017; 7.
21. Martinez-Lostao L, Anel A, Pardo J. How Do Cytotoxic Lymphocytes Kill Cancer Cells? Clin Cancer Res. 2015; 21 (22): 5047-5056.
22. Mojic M, Takeda K, Hayakawa Y. The Dark Side of IFN-γ: Its Role in Promoting Cancer Immunoevasion. Int J Mol Sci. 2017; 19 (1): 89.
23. Laidlaw BJ, Craft JE, Kaech SM. The multifaceted role of CD4(+) T cells in CD8(+) T cell memory. Nat Rev Immunol. 2016; 16:102.
24. Stanton SE, Disis ML. Clinical significance of tumor-infiltrating lymphocytes in breast cancer. J ImmunoTher Canc. 2016; 4 (1).
25. Lotfi A, Demarchi D, Puppo F, et al. Reliable redundancy with memristive-biosensors to achieve statistical significance in immunosensing. In 2015 6th International Workshop on Advances in Sensors and Interfaces (IWASI), 2015; pp 31-36.
26. Puppo F, Di Ventra M, De Micheli G, et al. Memristive sensors for pH measure in dry conditions. Surface Sci. 2014; 624: 76-79.
27. Vallero A, Tzouvadaki I, Puppo F, et al. Memristive Biosensors

Integration With Microfluidic Platform. IEEE Transactions on Circuits and Systems I: Regular Papers. 2016; 63 (12): 2120-2127.

28. Tzouvadaki I, Madaboosi N, Taurino I, et al. Study on the bio-functionalization of memristive nanowires for optimum memristive biosensors. J Mater Chem B. 2016; 4 (12): 2153-2162.
29. Tzouvadaki I, Aliakbarinodehi N, De Micheli G, et al. The memristive effect as a novelty in drug monitoring. Nanoscale. 2017; 9 (27): 9676-9684.
30. Ibberson M1, Bron S, Guex N, et al. TIE-2 and VEGFR kinase activities drive immunosuppressive function of TIE-2-expressing monocytes in human breast tumors. Clin Cancer Res. 2013; 19 (13): 3439-49.
31. Guex N, Crespo I1, Bron S, et al. Angiogenic activity of breast cancer patients' monocytes reverted by combined use of systems modeling and experimental approaches. PLoS Comput Biol. 2015; 11 (3): e1004050.
32. Bron S, Henry L, Faes-Van't Hull E, et al. TIE-2-expressing monocytes are lymphangiogenic and associate specifically with lymphatics of human breast cancer. Oncoimmunology. 2016; 5 (2): e1073882.
33. Gao A1, Lu N, Dai P, et al. Silicon-nanowire-based CMOS-compatible field-effect transistor nanosensors for ultrasensitive electrical detection of nucleic acids. Nano Letters. 2011; 11 (9): 3974-3978.
34. Jenkins RW, Aref AR, Lizotte PH, et al. Ex Vivo Profiling of PD-1 Blockade Using Organotypic Tumor Spheroids. Cancer Discov. 2018; 8 (2): 196-215.

To cite this article: Tuoheti A, Pabois A, Puppo F, et al. Immune Attack against Breast Cancer Revealed in Patient Tumor Sections by Memristive Nanowire Sensors. British Journal of Cancer Research. 2020; 3:1.